A driftwood-based record of Arctic sea ice during the last 500 years from northern Svalbard reveals sea ice dynamics in the Arctic Ocean and Arctic peripheral seas

Georgia Melodie Hole[1], Thomas Rawson[2], Wesley R. Farnsworth[3], Anders Schomacker[4], Ólafur Ingólfsson[3], and Marc Macias-Fauria[1]

[1]University of Oxford
[2]Imperial College London
[3]University of Iceland
[4]UiT The Arctic University of Norway

November 24, 2022

Abstract

We present a 500-year history of naturally felled driftwood incursion to northern Svalbard, directly reflecting regional sea ice conditions and Arctic Ocean circulation. Provenance and age determinations by dendrochronology and wood anatomy provide insights into Arctic Ocean currents and climatic conditions at a fine spatial resolution, as crossdating with reference chronologies from the circum-Arctic boreal forests enables determination of the watershed the driftwood originated from. Sample crossdating may result in a wide range of matches across the pan-boreal region, which may be biased towards regions covered by the reference chronologies. Our study considers alternate approaches to selecting probable origin sites, by weighting scores via reference chronology span and visualising results through spatiotemporal density plots, as opposed to more basic ranking systems. As our samples come from naturally felled trees (as opposed to logged, or both), the relative proportions of different provenances are used to infer past ocean current dominance. Our record indicates centennial-scale shifts in source regions for driftwood incursion to Svalbard, aligning with Late Holocene high variability and high frequency shifts in the Transpolar Drift and Beaufort Gyre strengths and associated fluctuating climate conditions. Driftwood occurrence and provenance also tracks the northward seasonal ice formation shift and migration of seasonal sea ice to the peripheral Arctic seas in the past century. A distinct decrease in driftwood incursion during the last 30 years matches the observed decline in pan-Arctic sea ice extent in recent decades. Our new approach successfully employs driftwood as a robust proxy for Arctic Ocean surface current and sea ice dynamics.

A driftwood-based record of Arctic sea ice during the last 500 years from northern Svalbard reveals sea ice dynamics in the Arctic Ocean and Arctic peripheral seas

Georgia M. Hole[1], Thomas Rawson[2], Wesley R. Farnsworth[3,4], Anders Schomacker[5], Ólafur Ingólfsson[4,6], Marc Macias-Fauria[1]

[1]Biogeosciences Research Group, School of Geography and the Environment, University of Oxford, Oxford, OX1 3QY, UK.

[2]Mathematical Ecology Research Group, Department of Zoology, University of Oxford, Oxford, OX1 3SZ, UK.

[3]Nordic Volcanological Center, University of Iceland, Sturlugata 7, IS-102 Reykjavík, Iceland

[4]Department of Arctic Geology, The University Centre in Svalbard (UNIS), NO-9171, Longyearbyen Norway

[5]Department of Geosciences, UiT The Arctic University of Norway, Postboks 6050 Langnes, NO-9037 Tromsø, Norway

[6]Faculty of Earth Sciences, University of Iceland, Sturlugata 7, IS-102 Reykjavík, Iceland

Corresponding author: Georgia M. Hole (georgiamhole@gmail.com)

Key Points

- We present a novel approach to utilizing naturally felled driftwood as a proxy for Arctic Ocean surface current and sea-ice dynamics.
- A 500-year record of driftwood incursion to northern Svalbard reflects Late Holocene variability in surface currents and climate conditions.
- A distinct decrease in driftwood in the last 30 years matches the observed decline in pan-Arctic sea-ice extent in recent decades.

Abstract

We present a 500-year history of naturally felled driftwood incursion to northern Svalbard, directly reflecting regional sea-ice conditions and Arctic Ocean circulation. Provenance and age determinations by dendrochronology and wood anatomy provide insights into Arctic Ocean currents and climatic conditions at a fine spatial resolution, as crossdating with reference chronologies from the circum-Arctic boreal forests enables determination of the watershed the driftwood originated from. Sample crossdating may result in a wide range of matches across the pan-boreal region, which may be biased towards regions covered by the reference chronologies. Our study considers alternate approaches to selecting probable origin sites, by weighting scores via reference chronology span and visualising results through spatiotemporal density plots, as opposed to more basic ranking systems. As our samples come from naturally felled trees (as opposed to logged, or both), the relative proportions of different provenances are used to infer past ocean current dominance. Our record indicates centennial-scale shifts in source regions for driftwood incursion to Svalbard, aligning with Late Holocene high variability and high frequency shifts in the Transpolar Drift and Beaufort Gyre strengths and associated fluctuating climate conditions. Driftwood occurrence and provenance also tracks the northward seasonal ice formation shift and migration of seasonal sea-ice to the peripheral Arctic seas in the past century. A distinct decrease in driftwood incursion during the last 30 years matches the observed decline in pan-Arctic sea-ice extent in recent decades. Our new approach successfully employs driftwood as a robust proxy for Arctic Ocean surface current and sea-ice dynamics.

Plain Language Summary

We present a 500-year history of driftwood arriving to the shorelines of northern Svalbard. Driftwood in the Arctic results from dying trees entering the large rivers that drain the circum-Arctic land masses, which upon flowing into the Arctic Ocean can then become locked up in forming sea-ice. This enables the wood to travel across the Arctic Ocean without sinking, making it an invaluable proxy for sea ice extent by recording variations in Arctic Ocean surface currents (and therefore sea ice drift) and ice cover. With comparison of tree ring width (TRW) measurements of these driftwood samples to TRW series from trees throughout the boreal forests, we can determine the region each sample came from via reconstructing its age and journey across the Arctic Ocean. Arctic sea ice is rapidly declining in extent and thickness, with impacts on local and global climatic and ecological conditions. Knowledge of past changes is needed to place this modern trend within a broader context to aid future predictions for Arctic sea ice. Our record matches the observational record of Arctic Ocean surface circulation patterns and climate conditions, therefore successfully evaluating driftwood as a proxy for Arctic Ocean surface current and sea-ice dynamics.

1. Introduction

The Arctic is a focal point for climatic changes on a range of temporal and spatial scales from geological to inter-annual, which makes the region a hotspot of warming under modern climate change due to the Arctic Amplification (Serreze & Francis, 2006) – a term for the feedbacks and interactions from the region's sea ice and snow cover resulting in enhanced and accelerated greenhouse gas-induced warming in the Arctic. Recent anthropogenic trends are well documented by a rapid decline in the extent and thickness of sea ice (Maslowski et al., 2012; Polyak et al., 2010). The continuing decline in sea-ice cover is expected to have a diverse range of consequences. These include a warmer and wetter Arctic, impacts on terrestrial and marine productivity, changes to global atmospheric and ocean circulation patterns, terrestrial fauna and flora population fragmentation and habitat reduction, increased marine species interaction and connectivity, and northward expansion of lower-latitude species (Bintanja & Andry, 2017; Bjorkman et al., 2020; Francis & Vavrus, 2012; Macias-Fauria & Post, 2018; Overland et al., 2016; Overland & Wang, 2010; Post & Høye, 2013; Screen & Simmonds, 2010, 2014; Vavrus et al., 2017). The Arctic Oscillation (AO) is defined as the principal component of extra-tropical Northern Hemisphere sea-level pressure and regarded as the most influential mode of atmospheric circulation and climate in the Arctic (Comiso & Hall, 2014; Thompson & Wallace, 1998). Dynamic processes affecting the Arctic Ocean such as the AO are being increasingly examined for their impact on ocean circulation and sea-ice dynamics (e.g. Barnes & Screen, 2015; Comiso & Hall, 2014; Ding et al., 2017; Hole & Macias-Fauria, 2017; Rigor et al., 2002). Data on past conditions are needed to understand the region's abiotic and biotic responses to various climatic processes and forcings and their resulting impacts on a global scale. Uncertainties remain on the spatiotemporal dynamics of Arctic sea ice throughout the Holocene, with limited, discontinuous data on sea-ice extent prior to the generation of spatially explicit sea-ice extent information by satellite observations in the late 1970s (Post & Høye, 2013). The observational record has been extended back in time to the late 19th century by compiling various observational data sources including ship reports, airplane surveys, compilations by naval oceanographers and analyses by national ice services (Walsh et al., 2017). Further knowledge of past sea ice dynamics is therefore needed to understand the context of recent change and gain insight into possible future sea ice trajectories under conditions of increasing global average temperatures.

1.1. The Arctic Ocean and sea-ice

The extent, thickness and dynamics of Arctic sea ice are driven by both thermal and physical dynamics of the Arctic Ocean system. These consist of many factors, with changes in ice extent, age and thickness driven by thermal processes such as the thermohaline circulation, surface warming and advection of warm waters. Physical dynamics include ocean and atmospheric circulations which influence the strength and position of the Arctic Ocean circulation patterns. Among these, the Beaufort Gyre (BG) and the Transpolar Drift (TPD) are the primary circulation systems in the modern Arctic. The two systems initiated during the Early Holocene after the closure of the Bering-Chukchi land bridge and opening of the Bering Strait *c.* 11 ka BP (Bartlein et al., 2015). The BG displays a mean annual clockwise motion in the western Arctic Ocean (Polyak et al., 2010), recirculating and enhancing survival of sea ice within the Arctic basin. The mean residence time for ice in the BG is c. 5 yr (Rigor et al., 2002), aiding the formation and preservation of multi-year ice that can reach up to 5 m thickness (de Vernal et al., 2013). The TPD is a surface ocean current running roughly parallel to the Siberian coast and transporting Arctic ice and waters southwards to the North Atlantic through the Fram Strait, favouring the loss of ice. Holocene fluctuations in the extent and orientation of the TPD have been proposed to vary between three overall states (Dyke et al., 1997). These involve lateral shifts from a) an eastward route toward Fram Strait, with sea ice (and any driftwood entrained in it) advection to the European Arctic; b) a westward route toward Greenland with sea ice advection to the Canadian Arctic Archipelago (CAA); and c) a split route with sea ice transport divided between the east and west. A driftwood-based reconstruction of the dynamics of Holocene sea ice extent and drift shows that there has been a progression from millennial to centennial shifts in the relative position of the TPD and BG throughout the Holocene (Hole & Macias-Fauria, 2017), consistent with the concurrent dynamics of the AO. The AO is a key physical driver of the position of the TPD and the balance between the strength of the BG and TPD circulation patterns. The AO Index is characterised as the variable atmospheric mass exchange between the Arctic Ocean and temperate latitudes (Rigor et al., 2002), with positive or negative polarity determined by anomalies in Sea Level Pressures (SLPs) over the polar regions and mid-latitudes (*c*. 55°–60°N; Kwok et al., 2013). The influence and variation in the AO over the Holocene is outlined in greater detail by Hole & Macias-Fauria (2017), including evidence of late Holocene centennial fluctuations in AO index polarity and ocean circulation patterns.

1.2. Sea-ice observations

Sea-ice observations provide information to varying degrees of accuracy, and the observational record encompasses – partially until the advent of remote sensing data – the past > 1,000 years. Since Iceland's settlement in c. 870 AD, records were kept of sea-ice incidence by Icelandic fisheries (Polyak et al., 2010), enabling a regional sea-ice index for the period A.D. 1600 – 1850 to be developed (Ogilvie & Jónsdóttir, 2000). In Svalbard, sea-ice information since 1800 has been collected from sealers, ships and trappers wintering on the archipelago by the Norwegian Polar Institute (Vinje, 2001). April sea-ice extent (a good proxy for maximum sea-ice extent) in the Nordic Seas from 1850–1998 has been generated from ship data, aircraft reconnaissance flights and satellite observation data (Vinje, 2001). In the Barents Sea, April sea ice was recorded by Norwegian ice charts by sealing and hunting expeditions from 1850-1949 and 1966-2001, and intervening years measured by Soviet reconnaissance aircraft (Shapiro et al., 2003). Sea-ice draft and thickness was also measured through upwards sonar data by submarine cruises throughout the Arctic from 1958 onwards (Rothrock et al., 2008). These include comparison of drift data from two summer polar cruises in 1958 and 1970 (McLaren, 1989), before more extensive draft data collection as part of the Scientific Ice Expeditions (SCICEX) program (Gossett, 1996). Since the 1970s, spatially explicit sea-ice extent information has been available by the development of satellite observations (Post & Høye, 2013). Using these records, Walsh et al. (2017) produced a spatially-explicit sea-ice dataset since the late 19th century at fine spatiotemporal resolution, enabling a comparison between historic data sets and proxy-based reconstructions (Post & Høye, 2013).

1.3. Reconstruction of past sea-ice conditions

The geological record and proxy data provide information on environmental and climatic conditions preceding the observational record. Raised beaches that occur in north-western Eurasia are an evident sign of postglacial adjustment of emergence following the retreat of past ice-sheet loads. Their current elevation results from the balance between eustatic sea level change and isostatic rebound of the lithosphere following the latest deglaciation of northern Eurasian ice sheets (Forman et al., 2004). Such raised beaches in Svalbard often lack vegetation due to their low temperatures, aridity, high alkalinity and low nutrient availability (Dyke et al., 1997; Forman et al., 2004). Such harsh conditions preserve datable driftwood, whalebones and pumice as decomposition is limited (Feyling-Hanssen & Olsson, 1959; Blake Jr, 1961; Bondevik et al., 1995; Schomacker et al., 2019; Farnsworth et al., 2020b). Driftwood is the preferred target for analysis in this study due to its terrestrial origin (and therefore radiocarbon dating suitability) and delivery to within 1-2 m above sea level by storm or ice pressure, although it can later migrate shoreward by slope processes (Funder et al., 2011).

Deposits of driftwood on Arctic shorelines reveal the transport by sea ice within large-scale Arctic Ocean circulations, which enables the reconstruction of past surface-current dynamics and sea-ice conditions in the Arctic (Dyke et al., 1997; Funder et al., 2011; Häggblom, 1982). Up to now, driftwood-inferred sea ice conditions have not been directly compared with the observational record. Reconstructions of past sea ice conditions employing this proxy have been based on an understanding of the conditions required for felled wood in the boreal forest to reach high arctic shorelines. The delivery of driftwood to the shores of Svalbard requires sea ice for long-distance transport due to its limited buoyancy once waterlogged (Häggblom, 1982), and seasonally open waters to enable wave action to deliver the driftage to the shoreline. The incurred driftwood derives from the major rivers that drain the boreal forest regions of North America and Eurasia and contribute 38% of the freshwater influx into the Arctic Basin (Serreze et al., 2006). In the high-latitude boreal forest zone, climate-mediated tree-growth is a common limiting factor, leading to coherency in tree-ring growth patterns within broad climatic region/watersheds (Ó Eggertsson, 1993). This coherency enables regional chronologies of mean tree-ring growth patterns to be created across the boreal forest zone (Schweingruber, 2012) and utilised for dendrochronological matching to driftwood derived from possible boreal source regions. Although the Arctic-draining rivers have been surrounded by boreal forest throughout the Holocene (Hopkins et al., 1981), the Eurasian boreal tree limit in the Early to Middle Holocene of c. 9.5-6 ka BP lay up to 200 km northwards at the circumpolar coastlines (MacDonald et al., 2000). This resulted from increased summer insolation and temperatures compared to modern conditions (MacDonald et al., 2008), which then migrated to the modern limit at 60-70°N (Bigelow et al., 2003; Sokolov et al., 1977). The boreal forest reached its current composition by *c.* 6 ka BP in Canada (Tremblay et al., 1997), and by 3-4 ka BP in Eurasia (MacDonald et al., 2000), with increased *Larix* occurrences during 10-3.5 ka BP.

The geographical distribution of tree species across the boreal forest (see MacDonald et al., 2008; Hellmann et al., 2013), has been used to make a genus-based division of driftwood sources to indicate wood provenance, with *Larix* assumed to indicate a Siberian origin, and *Picea* assumed to signify a North American origin (e.g. Dyke et al., 1997; Eggertsson, 1993; Funder et al., 2011; Häggblom, 1982; Hellmann et al., 2013; Nixon et al., 2016). For more spatially precise provenance determination, dendrochronology and tree ring width (TRW) analysis has proved a vital tool in dendroarchaeological efforts (Taylor & Aitken, 1997) and Arctic climatic and environmental reconstructions (Koch, 2009; Owczarek, 2010). Past driftwood dendrochronological studies have considered only reference chronologies associated with a particular drainage basin (Eggertsson, 1993; Eggertsson & Laeyendecker, 1995) based upon consideration of Arctic surface currents. However, some recent studies have highlighted that such assumptions can be incorrect, and a far wider extent of circumpolar sites must be considered during such processes, to accurately capture the potential history of samples (Hellmann et al., 2013). A recent combined assessment of radiocarbon and dendrochronological age estimates of Arctic driftwood samples (Sander et al., 2021) found that radiocarbon dates from buried driftwood were in agreement with dendrochronological dating of modern beach ridge systems in coastal eastern Siberia. This supports the validity of age indications obtained from driftwood found on Holocene beaches.

The aim of this paper is to utilise Arctic driftwood collected from modern shorelines to create a proxy-based reconstruction of regional sea-ice conditions and Arctic ocean circulation dynamics at a decadal resolution, and to evaluate inference made from naturally felled driftwood material against the observational record. In this study we provide a 500-year record of driftwood incursion onto northern Svalbard shorelines. TRW series and genus information is determined for the samples where possible, before crossdating with reference chronologies from the circum-Arctic boreal forest zone to determine of the climatic region/watershed the driftwood originated from. As sample cross-dating may result in a wide range of possible matches across the pan-boreal region and possible bias towards the regions covered by reference chronologies, our study includes a new approach to select most probable origin sites from multiple crossdating matches and visualising these results through spatiotemporal density plots. The resulting spatiotemporal distribution of best matches for all samples provides a 500-year time series of driftwood delivery to northern Svalbard, enabling a proxy-based reconstruction of Arctic Ocean surface current and sea-ice dynamics over this period. Our study confirms for the first time the validity of Arctic driftwood as a proxy for sea ice dynamics through the use of high spatial and temporal resolutions, achieved by employing modern wood samples and dendrochronological provenance with reference chronologies.

2. Methods

2.1. Sampling sites

The Svalbard archipelago is rich in raised beaches that preserve stranded driftwood. It is located at the proposed north-western part of the Late Weichselian Svalbard-Barents Sea Ice Sheet (SBSIS), with abundant preserved raised beach sequences reflecting the pattern and rate of relative sea level changes on Svalbard in response to the deglaciation of the SBSIS (Forman et al. 2004; Ingólfsson & Landvik, 2013). Samples were collected from three localities from the northern coastline of the Svalbard Archipelago and thus expected to collect driftwood from the same large-scale ocean currents (Fig. 1):

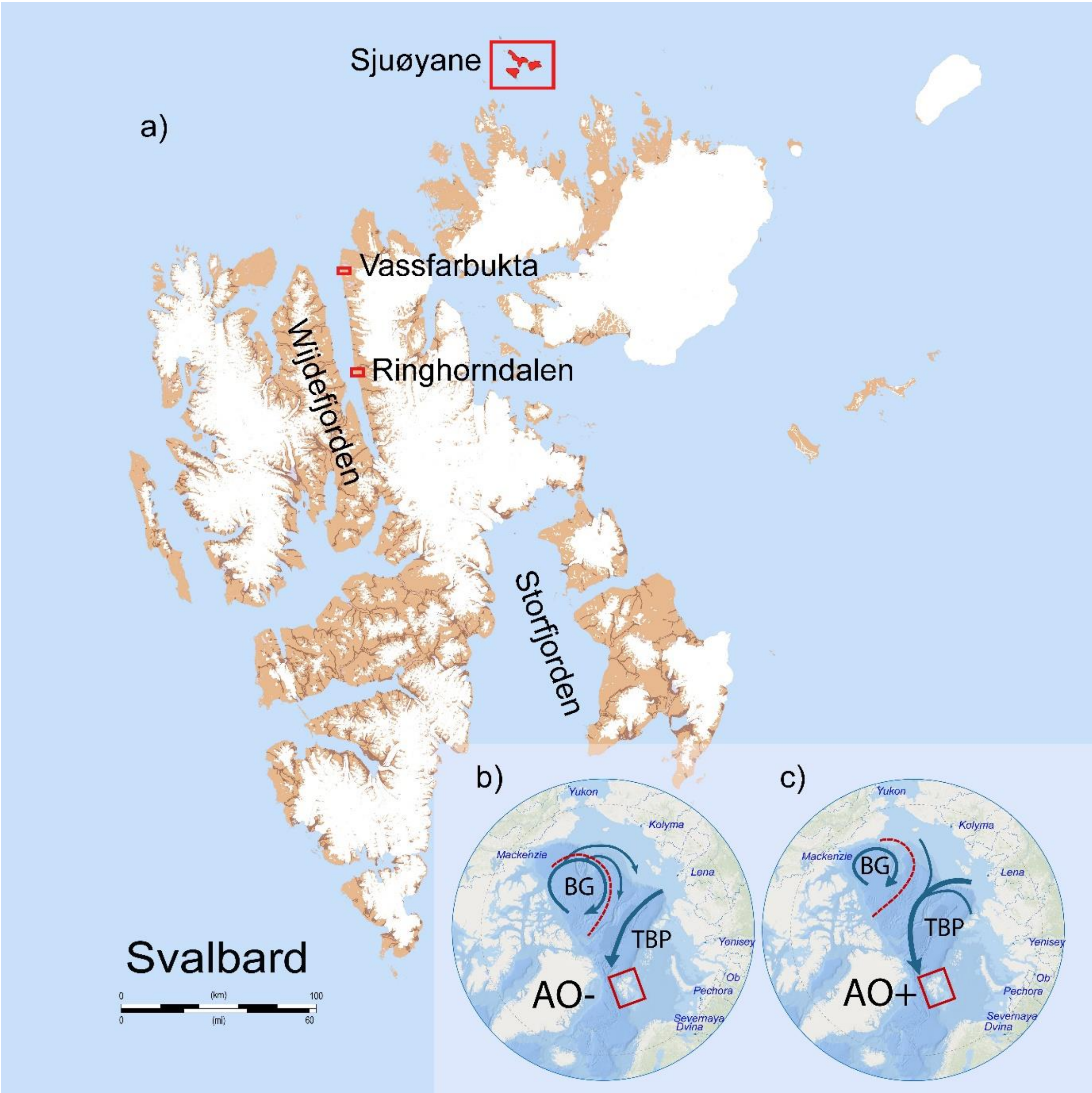

Figure 1 – a) Driftwood sampling locations of Sjuøyane, Ringhorndalen (sampled 2016), and Vassfarbukta (sampled 2018). Insert panel: Two modes of the Arctic Oscillation Index (AO), showing wintertime surface circulation patterns of Beaufort Gyre (BG) and Transpolar Drift (TBP), and the resulting influence on ice residence times. Map figure modified from Norwegian Polar Institute (2014). (b) Low index, negative AO polarity with a strengthened Beaufort Gyre and recirculation of sea ice. (c) High index, positive AO polarity with a weakened BG.The red dashed lines encircle the region of ice recirculation in the BG by the mean sea ice motion field (circulations compiled and modified from Rigor et al. (2002)).

Sjuøyane, an archipelago north of Nordaustlandet, and two localities within Wijdefjorden, northern Spitsbergen. On Sjuøyane, the lowlands above the marine limit are covered by glacial drift of angular to subangular cobbles and boulders, within a silty/clayey matrix. In this matrix there are abundant shell fragments, likely incorporated by glaciers originating from Nordaustlandet that also supplied erratics of granites and quartzites (Forman & Ingólfsson, 2000). Arrival and incursion of driftwood onto Sjuøyane and Wijdefjorden is influenced not only by broader ocean circulation dynamics and sea-ice conditions, but also by local deglaciation patterns and geomorphology. The deglaciation of Phippsøya occurred before *c*. 9.4 ka ago, with evidence from driftage dating and primary regressional strand deposits (Forman & Ingólfsson, 2000). The marine limit fell to ≤ current sea level *c*. 9-7 ka BP, before a transgression rising sea level to ≥ present levels at *c*. 6.2 ka BP indicated by cross-cutting beach ridges, and observed in other marginal foreland records around Svalbard such as a whalebone dated to *c*. 6 ka BP found at 5 m a.h.t., behind the modern storm beach of Kongsfjorden (Forman et al., 2004). The impact of such dynamics on driftwood incursion is minimal for this study, due to the aim to target samples from the modern shoreline for reconstruction of sea-ice conditions over recent centuries, and for the comparison of modern sample spatiotemporal distribution with observed circulation patterns and sea ice dynamics in the Arctic Ocean during the last 120 years.

2.2. Field sampling methods

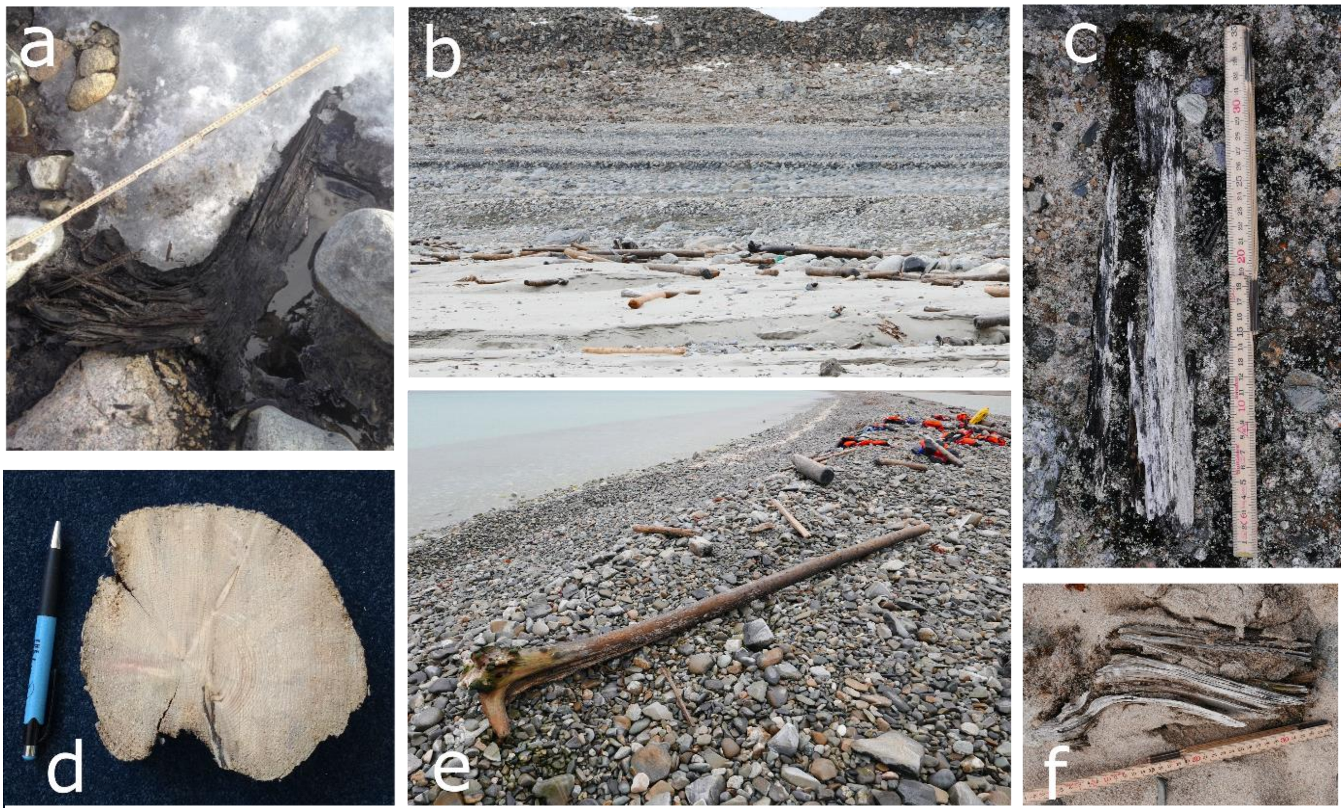

Figure 2. Range of preservation level of driftwood samples on Sjuøyane. Samples along the modern shoreline have the highest levels of preservation, with intact trunks and visible tree-ring series allowing dendrochronological analysis. Only samples that had sufficient preservation of tree rings and that preserved their root structure – and thus were likely naturally felled – were used to create our sample dataset (such as 2b, d, e). More degraded samples such as in 2a, c, f did not have sufficiently preserved rings to be included in the dataset.

A total of 95 driftwood samples were collected from Sjuøyane, Vassfarbukta and Ringhorndalen shorelines and raised beach terraces where samples were deemed in-situ. The datum for raised beach elevation measurements is the present mean high tide mark (m a.h.t.), seen at the coastline as a swash limit (Forman et al., 2004). The storm beach elevation can reach over 4 metres on bays exposed to direct storm fetch (Forman, 1990; Zeeberg et al., 2001) and this can carry washed up material substantially above the sea level of the time, giving uncertainties to dating by local geomorphological for raised-beach samples. Data were collected in August 2016 on the three largest islands of Sjuøyane (Martensøya, Phippsøya and Parryøya), Ringhorndalen in Wijdefjorden, Spitsbergen. At all sites, naturally felled driftwood at the modern shoreline was targeted by the sampling of logs exhibiting intact root stock. These driftwood logs were sub-sampled at peak thickness with a saw, where sub-sampled slices exhibited the maximum amount of intact tree-rings (Fig. 2). For elevation calculations, handheld GPS devices were used with occasional DGPS or altimeter data. Older driftwood was sparse, with most found ≤ 7 m a.h.t., and the majority of the samples are from the modern shoreline. During a July 2018 field campaign to Vassfarbukta in Wijdefjorden, Spitsbergen, a total of 30 samples were collected from driftwood deposited between the active beach face and the storm berm up to c. 4 m a.s.l. along a 200 m stretch of coast. Driftwood sampled varied in condition (Fig. 2), with modern samples having the best preservation (e.g., Fig. 2d) where tree rings would be intact enough for measurement.

2.3. Laboratory processing

Driftwood samples were assessed for viable tree ring series that are not dominated by individual growth anomalies. 59 of the 95 samples collected were found to have sufficient tree ring preservation for measurement and analysis. These were then sanded using drill-mounted sanding bands, and annual ring widths of each sample were measured to 1/1000 mm accuracy using LINTAB tree-ring measurement table and TSAP-Win Professional version 0.89 (Rinn, 2003). Samples also underwent microscopic genus identification where possible, through examination of stained radial, tangential and longitudinal sections. In the majority of dendrochronological studies, reference chronologies are limited to a specific temporal and geographical range based upon the context of the samples taken, be it by pre-existing knowledge of logging activity (Drake, 2018), or sapwood estimation (Daly, 2007; Hughes et al., 1981). Once a reference subgroup is determined, the “best match" is then identified as that with the highest t-value, a statistical measure of a sample’s similarity to a period in the reference chronology. Identifying such reference subgroups is a more difficult process when investigating naturally felled driftwood origins. The measured tree-ring series were cross-dated both visually by comparison of ring-width marker ring lists and by use of the chronology-building statistics of TSAP-Win software. Tree ring series were amassed and standardised to remove non-climatic trends such as ontogenetic growth and competition effects using a two-part trend elimination (Cook & Peters, 1997). The growth trend was removed through the application of a negative exponential curve or regression line, followed by detrending through a 5-year moving-average curve to remove further possible local variance. At least two radii per driftwood disc were measured and combined through a bi-weight robust estimate of the mean to form one chronology per sample.

2.4. Data Analysis

The 59 samples with sufficient measured time series were cross-dated using TSAP-Win using a variety of parameters to assess correlation between samples. Multiple scoring metrics have been utilised in assessing between-TRW time series similarity. A t-statistic is commonly employed to compare a sample set against a reference chronology, however to ensure the data are bi-variate normal the TRW are standardised by converting to a percentage of the mean of the five ring widths of which it is the centre value. This is then normalised by taking the natural log of percentage figures (Baillie & Pilcher, 1973). This de-trended value is referred to as TVBP, however the measure lacks descriptive power in the absence of extreme ring-differences between chronologies. For cases with less extreme ring-differences, the Gleichläufigkeit (Glk) parameter (or concordance coefficient) is also employed, which instead assesses similarity of sample slope intervals (Eckstein & Bauch, 1969; Schweingruber, 2012). To capture the strengths of both metrics, we consider the Cross-Date Index (CDI) within our study, provided by the TSAP-Win package (Rinn, 2003). CDI gives the quality of agreement between sample series by combining the Gleichläufigkeit measure of overall accordance of two series with the t-value measure of the correlation significance:

$$CDI = \frac{\left(G - 50 + \left(50 \times \sqrt{\frac{overlap}{\max overlap}}\right)\right) \times T}{10}$$

G is the Glk and T is the t-value, hence the CDI measure captures the magnitude of both measures Therefore, the combined CDI gives a date index of possible series matches (Rinn, 2003). Significant correlation was set to Glk >60%, TBP>3.0 and a CDI≥10 (Rinn, 2003). The cross-dating of series within the chronologies was examined using the COFECHA-style (Holmes, 1983) Cross-Date Check feature of TSAP-Win. Any series or segments of series that did not surpass sufficient cross-date parameters were removed. Series were combined to floating chronologies when possible and cross-dated with reference chronologies from the circum-Arctic boreal forest zone, sourced from the *International Tree Ring Data Bank* (ITRDB, http://www.ncdc.noaa.gov/data-access/paleoclimatology-data/datasets/tree-ring) (Grissino-Mayer & Fritts, 1997), providing possible age and source data for each driftwood sample.

In a first approach, all matches considered viable by TSAP-Win (CDI≥10) were plotted to display and investigate the spatiotemporal trend of matches, providing the density plots of the longitude and felling dates of all potential matches. However, since we consider a pan-boreal reference chronology, there is a risk of over-representing the geographic regions and time-periods that are better constrained by our reference chronology. That is, a sample may be more likely to match to a period/region for which there are more reference chronologies available. Figure 3 plots the longitude and timespan covered for each chronology within our reference chronology dataset. The grey-shaded y-axis density plot displays the distribution of longitudes represented, while the x-axis density plot depicts the distribution of how many chronologies cover each individual year. The geographic position is roughly evenly represented between the two key landmasses of the northern hemisphere. In terms of spatiotemporal coverage of reference chronologies, North America and Russia are better represented than Fennoscandinavia and north-eastern Europe. These regions are expected to contribute less driftwood due being regions without large Arctic-draining rivers, and so the sparsity of reference data in these regions are not anticipated to significantly impact crossdating trends. More recent years are also better represented by our reference chronology, which is also expected given the reliance of the database on the collection of reference chronology data.

Other dendrochronological studies that have considered a wider potential source region have demonstrated a wide range of t-value matches across the region, which would all have been considered a sign of good-fit by more restrictive references (Daly, 2007; Daly & Nymoen, 2008). Such studies will

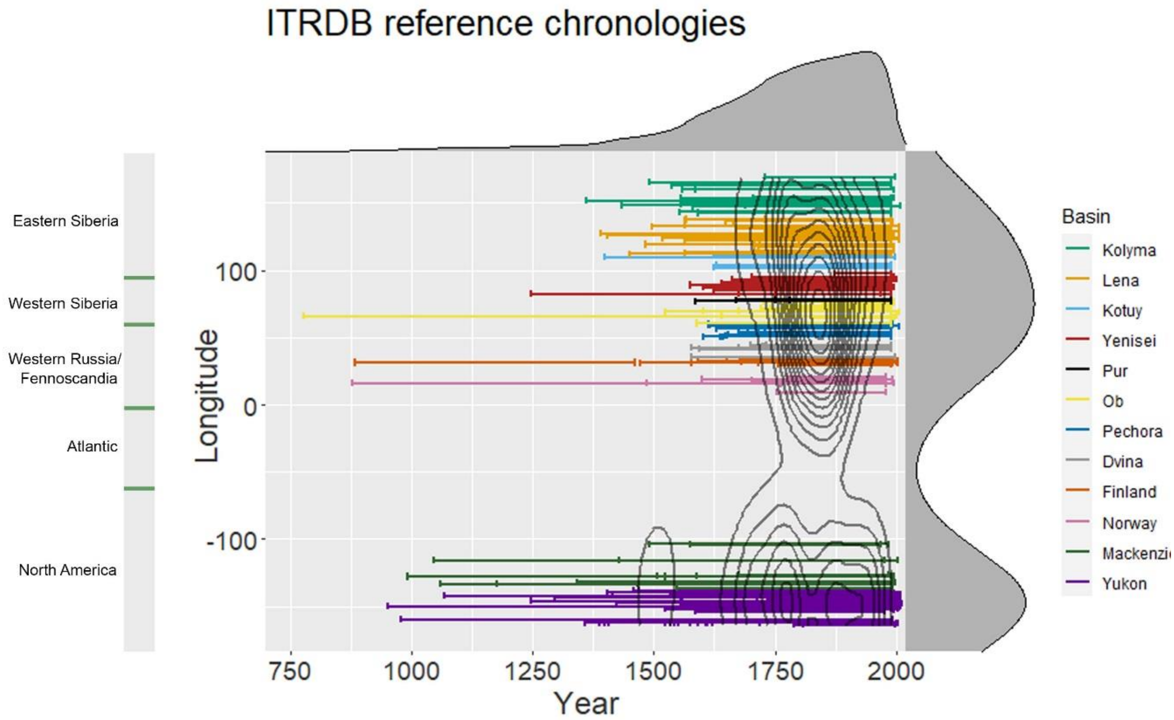

Figure 3. Spatiotemporal distribution of 222 reference chronologies from across the Eurasian and North American circum-Arctic boreal forest zone, sourced from the International Tree Ring Data Bank (ITRDB, http://www.ncdc.noaa.gov/data-access/paleoclimatology-data/datasets/tree-ring) (Grissino-Mayer & Fritts, 1997). Each line represents a single chronology, depicting the longitude and timespan covered, with line colours depicting the river basin/longitude of each chronology. The longitudinal density plot is directly calculated from the plotted longitudes, and the top density plot captures the number of chronologies that include the respective year. The overlaid contour plot is mapped using the longitudinal and time range midpoint data for each chronology.

still routinely use the highest t-value as a measure of the most probable origin, however such approaches risk bias towards regions with better developed reference chronologies. Based upon this, we computed a new metric ("Weighted Score") to help inform on of the most likely match within our results for each sample. This was achieved through weighting the CDI scores by the inverse of the density plots in Figure 3. As such, matches that are considered more "unlikely" by appearing in less-reported regions and time periods of the reference chronologies are rewarded. Additionally, the existence of the same temporal match for a sample to multiple chronologies strengthens the viability of these matches. As such, a new reference score is constructed for each potential match representing the initial CDI scores, corrected by the overall reference chronology spans, and increased by the number of identical temporal matches for the sample, i.e.:

$$Weighted\ Score = CDI\ \times \frac{(Total\ number\ of\ matches\ with\ the\ same\ timespan)}{Reference\ chronology\ densities\ for\ the\ match}$$

A match is considered better if it has a higher CDI and has multiple matches to the same timespan; plus, matches to a poorly represented region in the reference chronology are weighted positively. We next constructed linear interpolations of the reference chronology densities depicted in Figure 3 via the *approxfun* function within R. This produced two functions, $f_{time}(x)$, $f_{long}(y)$, which provide the relative densities for a given year x, and longitude y. We then calculated the new score for each match as:

$$Weighted\ Score = \frac{CDI\ \times n}{f_{time}(x) \times\ f_{long}(y) \times \sum^{matches} CDI}$$

where x and y are the start-date and longitude of the match in question, respectively. $matches$ is the total number of matches for the sample with the same start/end dates. n is the total of all match CDIs for the sample. In order to determine the 'best match' for each sample, the CDI values and Weighted Score values were examined, with high CDI values showing high Weighted Score values considered a sign of a good match. CDI scores, Weighted Scores and match choices are available in Supporting Information Dataset S2, and all match distribution plots for samples can be seen in the Supporting Information S3. All data processing, visualisation and score calculations are performed in *R* utilising the *tidyverse* suite of packages. All data and code used is made freely available at https://osf.io/z4t3a/.

3. Results

Of the 59 driftwood subsamples from northern Svalbard, 27% (16) are from the Seven Islands, while 73% are from Wijdefjorden (n=28 and n=15 from Ringhorndalen and Vassfarbukta respectively). Sample sites show no distinct variation of driftwood age, provenance or species (Fig. 5a). Segment lengths of series ranged from a minimum of 34 to a maximum of 281 years (see Fig. S1.1 in Supporting Information S1). Samples with greater segment length have more likelihood of cross-dating success with reference chronologies, and thus only a proportion of the samples are expected to be successfully

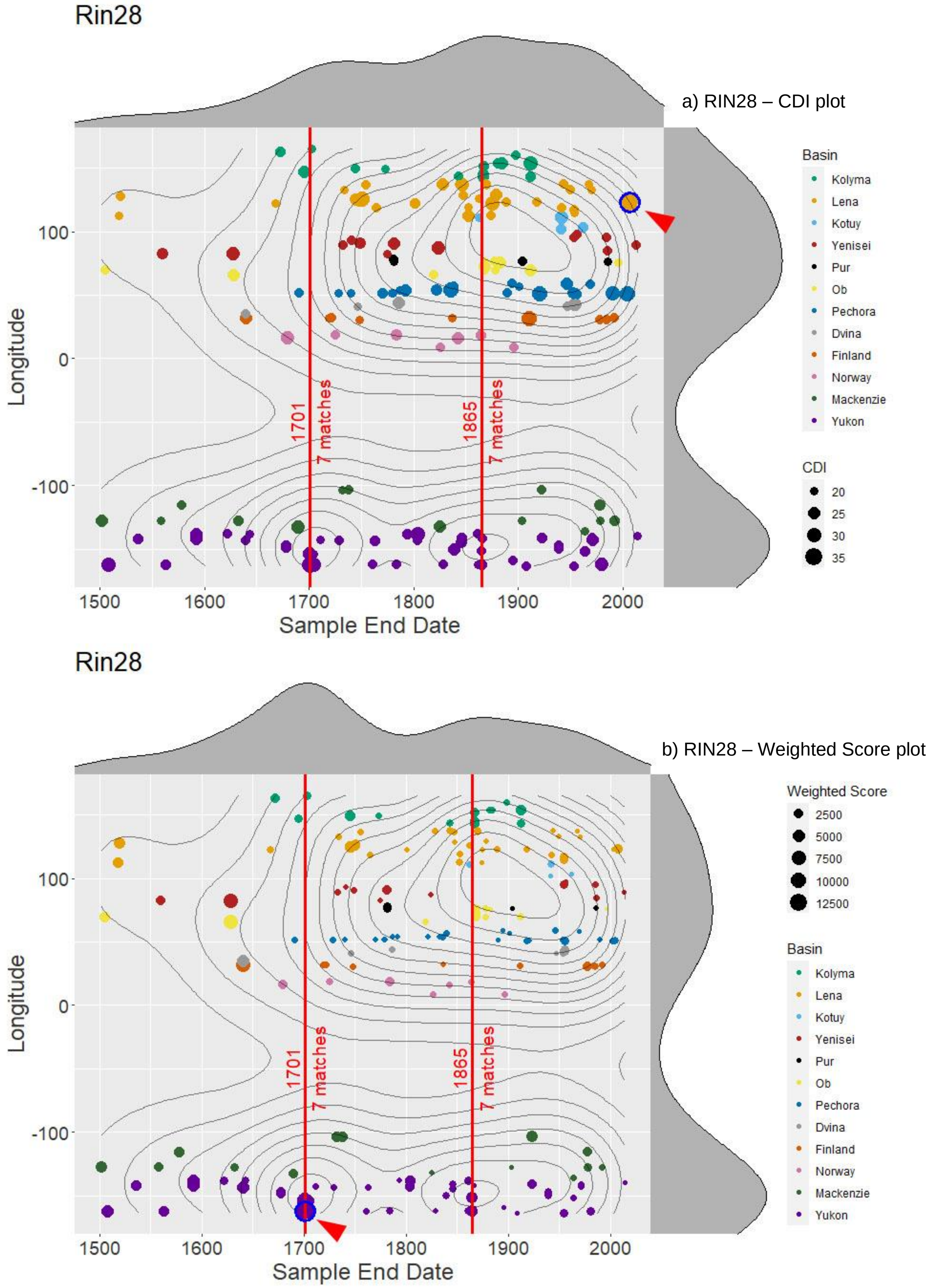

Figure 4. All potential matches for sample RIN28 using the scores CDI and Weighted Score. Each point represents a match to a chronology. The colour of the point displays the associated drainage basin, and the size of the point represents the CDI of the match in the upper plot and the Weighted Score in the lower plot. The density plots depict the densities of the associated time and longitude axes, weighted by the scores of the matches.

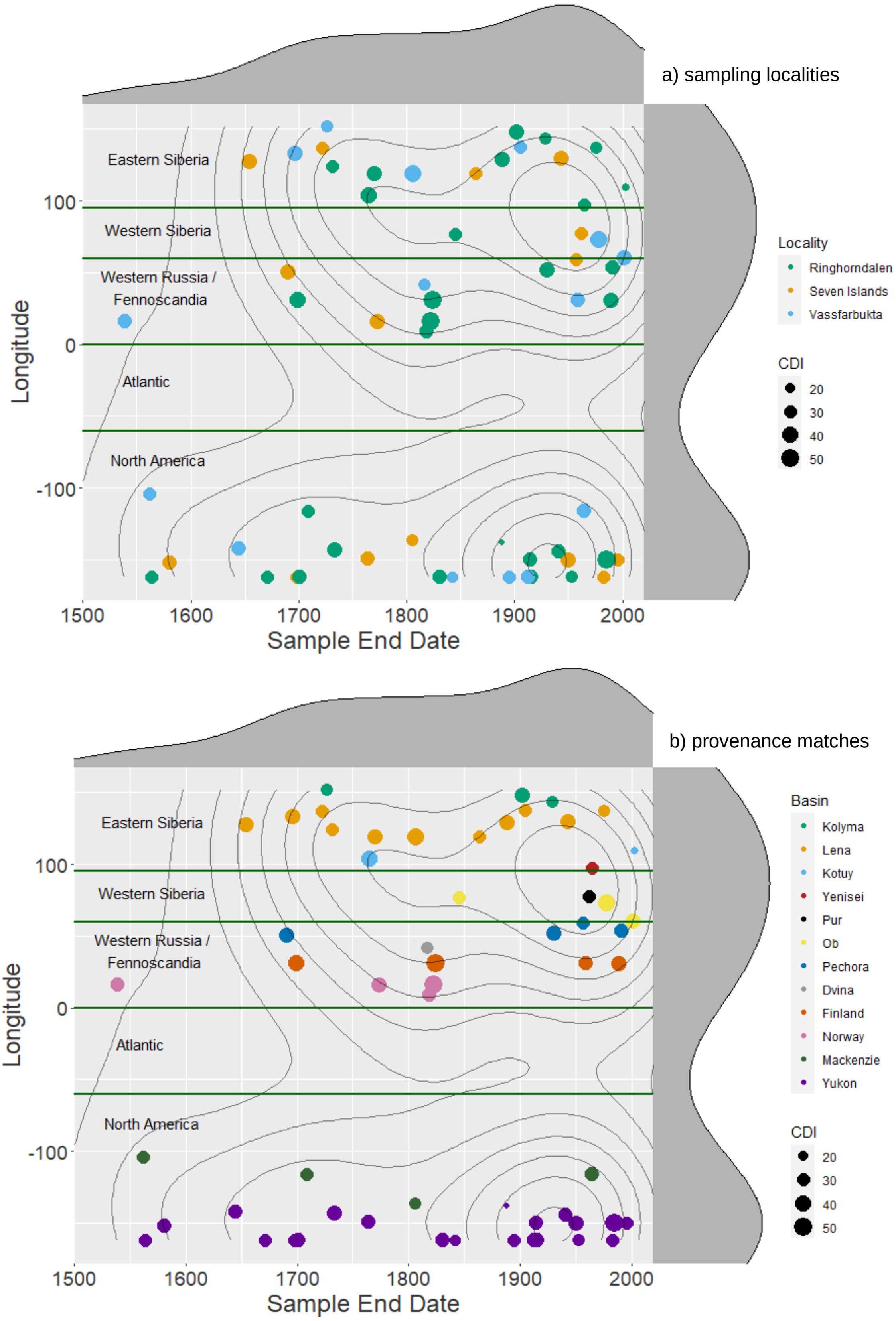

Figure 5. Plot of best matches for all samples. Each point represents a sample's best match to a chronology, with both matches included when a sample shows two possible matching chronologies (1 case – RIN40). a) The colour of each data point corresponds to the sampling site and the size of the point represents the CDI of the match b) The colour of each data point displays the associated drainage basin, and the size of the point represents the CDI of the match. The density plots depict the densities of the associated time and longitude axes, weighted by the CDI of the matches.

cross-dated and therefore have a provenance determined. All match plots are provided in Supporting Information S3, however we present in here the plot for one sample, RIN28, in Figure 4 to illustrate the method. RIN28 (segment length = 78 years) showed a high number of possible matches. Each point on the plot represents a potential match, where the colour of the point shows its associated drainage basin, and the size of the point represents the CDI value of the match. The density plots provided are constructed based upon the respective x and y value of each point and are weighted by the CDI value. If we were to follow the traditional approach of simply judging the highest t-value or CDI value as the best match, we would find the best match to be a fell date of 2007 from the Lena river region, longitude 123.36, with a CDI of 36 (highlighted by a blue circle and arrow in Fig. 4a). The year with the most concordance of common date matches is plotted in red, in this case 1701 or 1865 with 7 matches for each date. If we were to judge by the contour plot peaks of Figure 4a, we may instead conclude that a best match would be in the late 1800s from the Ob region. By utilising the Weighted Score metric, we can judge these factors together to find the most probable match in the face of all data, which we assess to be an end date of 1701 from the Yukon region via the crossdating match with the `Bye Rosanne/ak061' reference chronology in Alaska (highlighted with a blue circle and arrow in Fig. 4b).

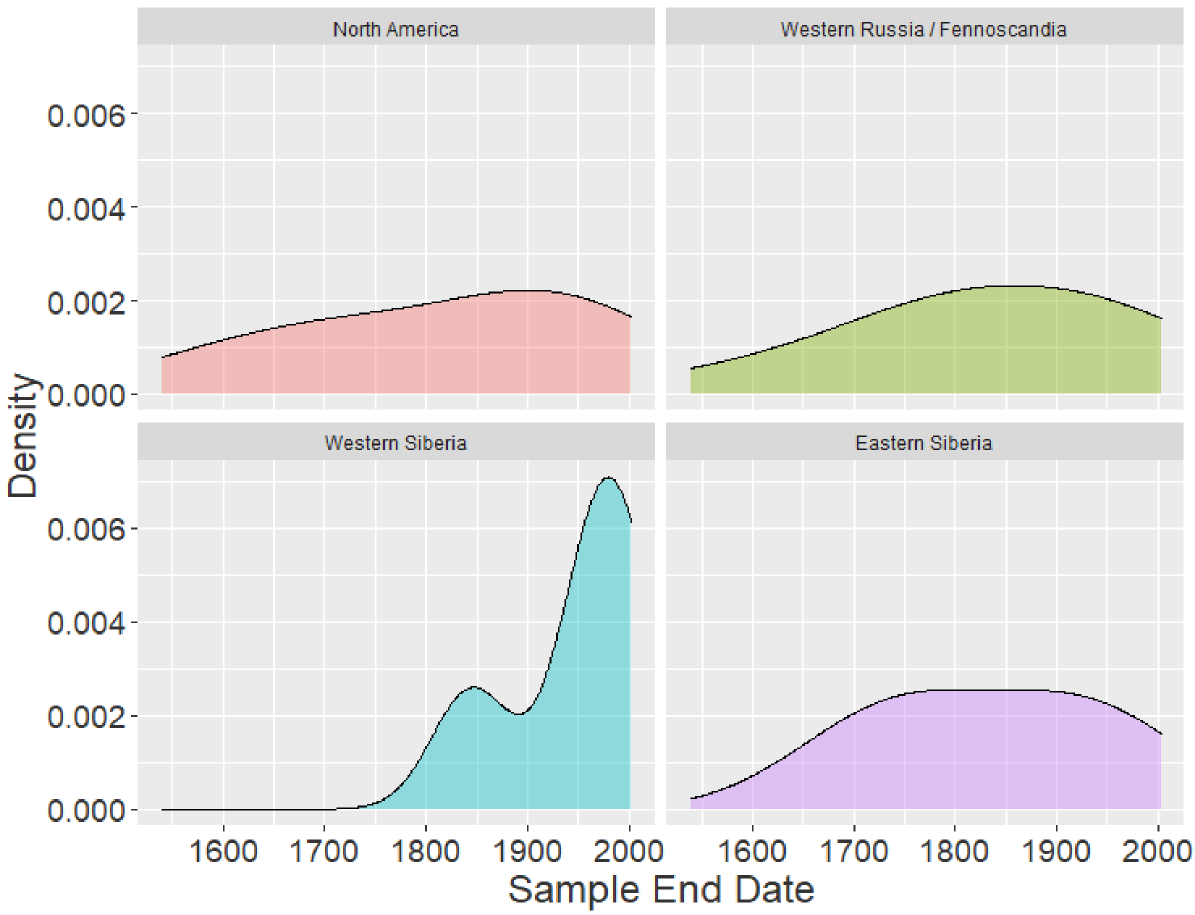

Figure 6. Plot of best match density plots for the four regions North America, Western Russia/Fennoscandia, Western Siberia, and Eastern Siberia, matching regions shown in Figure 5. The density plots depict the densities of the associated time and longitude axes, weighted by the CDI of the matches.

All best matches and weighted scores, with rationale behind match choices via this method, are available in Supporting Information S2.

After having assessed the most likely matches for each sample, we plot these combined best matches in Figure 5, with two matches included when a sample shows two possible matching chronologies (this was only required for one sample – RIN40). The CDIs for each match is shown in Fig. 5 due to the inter-sample comparability, whereas the Weighted Scores values consist of a more variable magnitude making comparison between samples less useful than comparison of scores per sample. Plots of best matches divided by sampling locality (Seven Islands, Ringhorndalen and Vassfarbukta) are available in Supporting Information S1 and show a consistent trend across the three localities. Regional density plots are then also shown in Figure 6, with the regional divisions as depicted in Figure 5. Examination of the spatiotemporal distribution of these samples reveals centennial-scale shifts in the contributing sources of Arctic Driftwood to northern Svalbard and the contemporaneous ocean circulation patterns and sea-ice distribution that enable their transport across the Arctic Ocean. Such trends will be discussed in relation to the observational record in the following section.

4. Discussion

The data show (Figures 5 & 6) that the proportion of Siberian driftwood arriving in Svalbard is greater than that from North American regions as a whole, as expected due to a greater number of boreal zone-draining rivers. These findings agree with both observations (e.g., (Hellmann et al., 2017), although in that case the samples contained both naturally felled and logged material) and modelling of driftwood transport based on sea ice velocity, concentration and the sea surface current velocity (Dalaiden et al., 2018). A lack of samples arriving before 1650 from Siberian origin correlates to the period of low Arctic sea ice cover that spanned the 16^{th} and early 17^{th} centuries (T2 in the multiproxy reconstruction by Kinnard et al., 2011, that did not employ driftwood). Driftwood delivery (and thus inferred sea ice extent) increased markedly in the subsequent ~150 years (again, in line with Kinnard et al. 2011), with a mixed arrival of both Eurasian and North American driftwood between 1700 and 1850, suggesting a well-developed BG able to deliver North-American wood to Svalbard entrained in the TPD. There is a notable halt of Western/Russian Fennoscandian driftwood delivery after 1850 (Figure 5): for this material to arrive on the northern shores of Svalbard, sea ice is required in the Barents sea, which will carry it north / north-eastwards towards the Arctic Ocean before joining the TDP. While wood from North-eastern Europe will resume its arrival to Svalbard again in mid-20^{th} century, we only report wood material from Norway during the period 1750-1850, suggesting sea ice in the southern Barents Sea. There is a lack of driftwood originating from the most eastern Siberian sources such as the Kolyma basin between 1750 and 1900. This may be indicative of the trajectory of such distal driftwood sources. Given the mean residence time of ice from North America and far-eastern Russia region is *c.* 5 years (Rigor et al., 2002), there is the possibility of entrainment into the Beaufort Gyre disrupting travel to northern Svalbard, or seasonal sea-ice formation focused in the Barents Sea region, favouring driftwood delivery from this region. The rates of change in the primary ocean circulations and AO mode during this period also correlate with the temporal and regional heterogeneity of these periods across the Arctic and beyond (Jones & Mann, 2004), with sea ice-ocean feedbacks amplifying the climatic transitions during this period (Lehner et al., 2013).

Further information from direct observations of sea-ice dynamics is available for the last 120 years and can be compared to the driftwood record to assess the accuracy of driftwood temporal distribution reflecting the known conditions of the time. A composite historical record of Arctic sea ice margins from 1870-2003 shows a trend of retreat in seasonal ice 1900 onwards, with acceleration of seasonal and annual ice retreat during the last five decades with spatially-variable sea-ice distribution changes across the Arctic (Kinnard et al., 2008). Seasonal sea-ice was comparatively more frequent in the southern portion of the Barents and Greenland-Iceland-Norwegian (GIN) Sea and less frequently in the Eurasian coastal region during the late 19th and early 20th centuries. This might be reflected in the perceived dip in the delivery of Western Siberian driftwood around that time (Figure 6) and in the lack of driftwood material from Western Eurasia in general (Figure 5). Additionally, a reconstruction of Western Nordic Seas maximum sea ice indicates a minima in sea ice extent in the 1920s and 1930s (Macias-Fauria et al., 2010). There is further evidence of such conditions favouring reduced ice, with atmospheric warming driven by enhanced atmospheric and ocean heat transport from the North Atlantic into the region from 1900 to 1940 (Bengtsson et al., 2004; Vinje, 2001). The decline in driftwood delivery to northern Svalbard arriving from Western Russian/Fennoscandian sources after the 1850s may be an indication of a reduction of sea ice in the Barents Sea in this period, as indicated by a sustained reduction in March and September ice extent time series from 1850 - 2013 (Walsh et al., 2017). The increase in September sea ice during the late mid-20th century, reaching a relative maximum by the 1970s, within a framework of strong decadal and multidecadal variability on a regional basis, is seen in a peak in Western Siberian driftwood delivery in the latter half of the 20th century in contrast to decreases for other regions (Fig. 6), indicating the favouring of proximal sources of driftwood from Eurasian coasts in this period. The steady – even centennial – increase in the delivery of North-American driftwood until recent decades likely reflects North-American continent being a more stable (i.e., less variable) source of driftwood in recent centuries, in agreement with a much higher sea ice variability in the Eurasian marginal Arctic seas (most notably the Barents Sea). As a consequence, increases in the overall frequency of North American wood delivery in Svalbard can signal, depending on the context, lack of sea ice on the Eurasian marginal seas.

Finally, there is a distinct decrease in driftwood incursion during the last 30 years from all regions (Fig. 6), indicating a lack of sufficient multi-year sea-ice throughout the Arctic to raft driftwood to Svalbard shorelines, matching the record of systematic post-1970 decrease in pan-Arctic sea-ice extent (Walsh et al., 2017). For the period 1990-2003, records show the trend continues with an Arctic-wide retreat of the summer ice cover resulted in a net increase in the extent, and a migration of seasonal sea-ice to the peripheral Arctic seas (Kinnard et al., 2008; Walsh et al., 2017). This spatial shift is matched with multi-year ice loss and replacement with first-year ice, with resulting reduction in driftwood-carrying potential expected to affect the most recent driftwood incursion rates. The most recent matched dates for our driftwood record are 3 samples matched to dates 1991-1996, originating from eastern Eurasia and the Yukon drainage basins, which given the average travel time of up to 7 years for Arctic driftwood (Häggblom, 1982), indicates some continued influx of driftwood at this time but insufficient data to confidently correlate with observational data for the most recent decade. These results are even more remarkable given the ample availability of reference dendrochronologies for this period.

These centennial-scale shifts in source regions for driftwood incursion to Svalbard align with Late Holocene high variability and high frequency shifts in the TPD and BG strength and associated fluctuating climate conditions as found with previous driftwood-based reconstruction of Holocene Arctic Ocean surface current and sea ice dynamics (Hole & Macias-Fauria, 2017). A recent study of 380 driftwood samples collected on eastern and south-western Svalbard (Linderholm et al., 2021) found a dominance (87%) in driftwood originating from northern Russia, with samples dated to the nineteenth and twentieth centuries which were periods of high logging activity in Russia. The study incorporates logged wood which is subject to anthropogenic influence on trends that reflect the logging activity at the time of their harvesting (Hellmann et al., 2016). Therefore a direct comparison is not applicable to our spatiotemporal record which targets naturally felled wood only. Other proxy-based reconstructions of sea ice, such as those derived from the IP_{25} biomarker, also suggest variability in sea-ice cover during the Late Holocene associated with intermittent warm sea surface temperatures (Allaart et al., 2020; Jernas et al., 2013; Müller et al., 2012; Pawłowska et al., 2020; Sarnthein et al., 2003). Records of brine formation can be interpreted as a proxy for sea-ice cover above basins, with a varied Late Holocene record from Storfjorden (Fig. 1) suggesting episodic fluctuations between intense and reduced brine formation and concurrent sea-ice cover variability (Rasmussen & Thomsen, 2014). A reconstruction of maximum sea ice extent in the Western Nordic Seas based upon tree ring chronologies and ice core ocxygen isotopes (Macias-Fauria et al., 2010) again show such variability, including the sea-ice maxima during the LIA, and of record strong overall 20th century decline.

4.1 Sources of Uncertainty

The utilisation of the Weighed Score aids in reducing the bias of varied spatiotemporal coverage of the reference chronology, but sources of uncertainty do remain when interpreting the record. Late Holocene transgression may influence the preservation of older samples (Forman et al., 2004; Farnsworth et al., 2020a). Degraded samples not included in the tree ring width dataset (Fig. 2) may have implications for observed Arctic driftwood densities, although these were predominantly observed at higher elevations than our target sampling sites at the modern day shoreline, suggesting older ages, and were often found from melting snowbanks and hence very moist. The impact of possible degraded samples is likely more relevant for the earliest centuries of the dataset. Given these more heavily degraded samples cannot be cross-referenced to our reference chronology and dated, the ages of these ~30 samples are unknown. Therefore, when interpreting the contrasting regional trends in the earlier years of our dataset (Fig. 6), we assume that driftwood degradation is a risk equally applicable to all samples irrespective of their origin. Local sea-ice conditions must also be considered when intrepreting the driftwood record from these Svalbard collection sites, as persistent or semi-permanent land-fast ice resulting from localised cold conditions would minimize the transport of and catchment for driftwood accumulation (Funder et al., 2011), especially when considering that our sample sites are in the northernmost part of the archipelago.

Another feature to consider when utilising and interpreting driftwood as a proxy for sea-ice dynamics is the impact that fcircumpolar rivers flow regimes that transport this wood from boreal forest zones might have had on driftwood delivery to the Arctic basin. Wohl et al. (2019) summarise these processes, whereby characteristics of flow are the first-order controls on wood transport, while spatial and temporal variation in channel and floodplain geometry, sediment inputs and mobility, wood piece size, and wood storage (e.g., dispersed pieces versus jams) all influence wood transport. Variation in outflow and its impacts on sea ice also has an impact on driftwood transport (Park et al., 2020), with potential to be a factor influencing the observed decline in the last three decades as riverine heat influx has increased. Therefore, the survival and time delay between a boreal forest tree falling into a cirumpolar river and entering the Arctic Ocean will be impacted by conditions affecting wood entrainment into channel margins and downstream transport such as channel size (Gregory et al., 2003), local flow regime and flow width and depth (Kramer & Wohl, 2017) and channel–floodplain connectivity (Wohl et al., 2018). Temporal factors such as spring melt, storms and flooding impacts these features and so also impacts downstream flow and ocean entry. Given the centennial spatiotemporal scope of the dataset, and lack of sufficient available data on these variety of factors for the pan-Arctic across the past 500 years, these impacts are assumed not to have had a substantial impact on the trends observed.

5. Conclusions

We present a 500-year history of driftwood incursion to Northern Svalbard reflecting associated sea-ice and Arctic ocean circulation and provide for the first time a direct evaluation of sea ice dynamics inferred from naturally felled driftwood against the observational record. By crossdating samples against a circumpolar reference chronology across North American and Eurasian boreal forest zone drainage basins, a wide range of statistically significant matches can occur across the region, which would be considered a sign of good-fit by more restrictive references. To minimise the risk of bias towards regions covered by more reference chronologies, our study employs a novel approach to selecting probable origin sites, by weighting matches via reference chronology span and visualising results through spatiotemporal density plots. Our spatiotemporal record of driftwood incursion to northern Svalbard indicates centennial-scale shifts in driftwood source regions, aligning with Late Holocene high variability and high frequency shifts in the TPD and BG strength and associated fluctuating climate conditions, and northward seasonal ice formation shift and migration of seasonal sea-ice to the peripheral Arctic seas in the past century. In particular, we find that the increased spatio-temporal grain of the provenance of driftwood material informs not only about the relative contributions of the TDP and the Beaufort Gyre (as in Funder et al., 2011), but also about the presence – or lack thereof – of sea ice in Arctic Marginal seas key to the global circulation (e.g., the Barents Sea), and of the overall sea ice conditions in the Arctic peripheral seas in general. A distinct decrease in driftwood incursion during the last 30 years matches the observed decline in pan-Arctic sea-ice extent in recent decades, further highlighting the sensitivity of this unique sea ice proxy.

6. Author Contributions

GMH and MMF conceived this work. GMH authored the paper with contributions from all co-authors. All authors contributed with literature compilation, data interpretation and the discussion of results. This study is based on data collected in collaboration with the University Centre in Svalbard (UNIS), with the field campaign to Sjuøyane, training and logistics provided and funded by UNIS. The 2016 fieldwork was completed with sample collection by GMH and MMF across Sjuøyane in collaboration with the field course cohort. The samples from Ringhorndalen, Wijdefjorden were collected in 2016 by MMF and WRF, and from Vassfarbukta in 2018 by WRF and S. Brynjolfsson.

7. Acknowledgments

This work was supported by the UK Natural Environmental Research Council (NERC IRF grant: NE/L011859/1). GMH is funded by NERC (grant: 1514291) and part of the Environmental Research Doctoral Training Program at the University of Oxford. Support and funding were also provided by MMF and grant funds from the Natural Environment Research Council (NERC). TR is supported through an Engineering and Physical Sciences Research Council (EPSRC) (https://epsrc.ukri.org/) Systems Biology studentship award (EP/G03706X/1). Thanks to S. Brynjolfsson for assistance in sample collection during 2016 and 2018 at Wijdefjorden locations and to L. Allaart for leading funding of the 2018 field campaign to Vassfarbukta. The Wijdefjorden field campaigns in 2016 and 2018 were funded by grant numbers 16/35 (to WRF) and 17/01132-3 (to LA) from the Svalbard Environmental Protection Fund respectively, Arctic Field grant no. 282643 awarded to LA by Svalbard Science Forum/Research Council of Norway, and the Arctic Research and Studies Program of the Ministries for Foreign Affairs of Norway and Iceland (grant agreement No. 2017-ARS-79772 to AS).

8. Data Availability Statement

All data used in this study are available at https://osf.io/z4t3a/.

9. References

Allaart, L., Müller, J., Schomacker, A., Rydningen, T. A., Håkansson, L., Kjellman, S. E., et al. (2020). Late Quaternary glacier and sea-ice history of northern Wijdefjorden, Svalbard. *Boreas*, *49*(3), 417–437. https://doi.org/10.1111/bor.12435

Baillie, M., & Pilcher, J. (1973). A simple crossdating program for tree-ring research. *Tree Ring Bulletin*. https://doi.org/S

Barnes, E. A., & Screen, J. A. (2015). The impact of Arctic warming on the midlatitude jet-stream: Can it? Has it? Will it? *Wiley Interdisciplinary Reviews: Climate Change*, *6*(3), 277–286. https://doi.org/10.1002/wcc.337

Bartlein, P. J., Edwards, M. E., Hostetler, S. W., Shafer, S. L., Anderson, P. M., Brubaker, L. B., & Lozhkin, A. V. (2015). Early-Holocene warming in Beringia and its mediation by sea-level and vegetation changes. *Climate of the Past*, *11*(9), 1197–1222. https://doi.org/10.5194/cp-11-1197-2015

Bengtsson, L., Semenov, V. A., & Johannessen, O. M. (2004). The early twentieth-century warming in the Arctic—A possible mechanism. *Journal of Climate*, *17*(20), 4045–4057.

Bigelow, N. H., Brubaker, L. B., Edwards, M. E., Harrison, S. P., Prentice, I. C., Anderson, P. M., et al. (2003). Climate change and Arctic ecosystems: 1. Vegetation changes north of 55 N between the last glacial maximum, mid-Holocene, and present. *Journal of Geophysical Research: Atmospheres*, *108*(D19).

Bintanja, R., & Andry, O. (2017). Towards a rain-dominated Arctic. *Nature Clim. Change*, *7*(4), 263–267. Retrieved from http://dx.doi.org/10.1038/nclimate3240

Bjorkman, A. D., García Criado, M., Myers-Smith, I. H., Ravolainen, V., Jónsdóttir, I. S., Westergaard, K. B., et al. (2020). Status and trends in Arctic vegetation: Evidence from experimental warming and long-term monitoring. *Ambio*, *49*(3), 678–692. https://doi.org/10.1007/s13280-019-01161-6

Blake Jr, W. (1961). Radiocarbon Dating of Raised Beaches in Nordaustlandet, Spitsbergen. In G. O.

Raasch (Ed.) (pp. 133–146). University of Toronto Press. https://doi.org/doi:10.3138/9781487584979-010

Bondevik, S., Mangerud, J., Ronnert, L., & Salvigsen, O. (1995). Postglacial sea-level history of Edgeøya and Barentsøya, eastern Svalbard. *Polar Research*, *14*(2), 153–180.

Comiso, J. C., & Hall, D. K. (2014). Climate trends in the Arctic as observed from space. *Wiley Interdisciplinary Reviews: Climate Change*, *5*(3), 389–409. https://doi.org/10.1002/wcc.277

Cook, E. R., & Peters, K. (1997). Calculating unbiased tree-ring indices for the study of climatic and environmental change. *Holocene*, *7*(3), 361–370. https://doi.org/10.1177/095968369700700314

Dalaiden, Q., Goosse, H., Lecomte, O., & Docquier, D. (2018). A model to interpret driftwood transport in the Arctic. *Quaternary Science Reviews*, *191*, 89–100. https://doi.org/https://doi.org/10.1016/j.quascirev.2018.05.004

Daly, A. (2007). The Karschau ship, Schleswig-Holstein: Dendrochronological results and timber provenance. *International Journal of Nautical Archaeology*, *36*(1), 155–166.

Daly, A., & Nymoen, P. (2008). The Bøle ship, Skien, Norway—Research history, dendrochronology and provenance. *International Journal of Nautical Archaeology*, *37*(1), 153–170.

Ding, Q., Schweiger, A., Battisti, D. S., Johnson, N. C., Wrigglesworth, E. B., Zhang, Q., et al. (2017). Influence of the recent high-latitude atmospheric circulation change on summertime Arctic sea ice, (March). https://doi.org/10.1038/NCLIMATE3241

Drake, B. L. (2018). Source & Sourceability: Towards a probabilistic framework for dendroprovenance based on hypothesis testing and Bayesian inference. *Dendrochronologia*, *47*, 38–47.

Dyke, A. S., England, J. H., Reimnitz, E., & Jetté, H. (1997). Changes in driftwood delivery to the Canadian Arctic Archipelago: The hypothesis of postglacial oscillations of the transpolar drift. *Arctic*, *50*(1), 1–16.

Eckstein, D., & Bauch, J. (1969). Beitrag zur Rationalisierung eines dendrochronologischen Verfahrens und zur Analyse seiner Aussagesicherheit. *Forstwissenschaftliches Centralblatt, 88*(1), 230–250. https://doi.org/10.1007/BF02741777

Eggertsson, Ó. (1993). Origin of the driftwood on the coasts of Iceland; a dendrochronological study. *Jökull*, *43*(JANUARY 1993), 15–32.

Eggertsson, Ólafur, & Laeyendecker, D. (1995). A dendrochronological study of the origin of driftwood in Frobisher Bay, Baffin Island, NWT, Canada. *Arctic and Alpine Research, 27*(2), 180–186.

Farnsworth, W. R., Blake Jr, W., Guðmundsdóttir, E. R., Ingólfsson, Ó., Kalliokoski, M. H., Larsen, G., et al. (2020). Ocean-rafted pumice constrains postglacial relative sea-level and supports Holocene ice cap survival. *Quaternary Science Reviews*, *250*, 106654. https://doi.org/https://doi.org/10.1016/j.quascirev.2020.106654

Feyling-Hanssen, R. W., & Olsson, I. (1959). Five radiocarbon datings of Post Glacial shorelines in Central Spitsbergen. *Norsk Geografisk Tidsskrift - Norwegian Journal of Geography, 17*(1–4), 122–131. https://doi.org/10.1080/00291955908551761

Forman, S. L. (1990). Post-glacial relative sea-level history of northwestern Spitsbergen, Svalbard. *Geological Society of America Bulletin*, *102*(11), 1580–1590.

Forman, S. L., & Ingólfsson, Ó. (2000). Late Weichselian glacial history and postglacial emergence of Phippsøya, Sjuøyane, northern Svalbard: a comparison of modelled and empirical estimates of a glacial-rebound hinge line. *Boreas*, *29*(1), 16–25. https://doi.org/10.1111/j.1502-3885.2000.tb01197.x

Forman, S. L., Lubinski, D. J., Ingólfsson, Ó., Zeeberg, J. J., Snyder, J. A., Siegert, M. J., & Matishov, G. G. (2004). A review of postglacial emergence on Svalbard, Franz Josef Land and Novaya Zemlya, northern Eurasia. *Quaternary Science Reviews, 23*(11–13), 1391–1434. https://doi.org/10.1016/j.quascirev.2003.12.007

Francis, J. a, & Vavrus, S. J. (2012). Evidence linking Arctic amplification to extreme weather in mid-latitudes, *39*(February), 1–6. https://doi.org/10.1029/2012GL051000

Funder, S., Goosse, H., Jepsen, H., Kaas, E., Kjær, K. H., Korsgaard, N. J., et al. (2011). A 10,000-Year Record of Arctic Ocean Sea-Ice Variability—View from the Beach. *Science*, *333*(6043), 747–750. https://doi.org/10.1126/science.1202760

Gossett, J. (1996). Arctic research using nuclear submarines. *Oceanographic Literature Review*, *43*(11), 1171.

Gregory, S., Boyer, K. L., & Gurnell, A. M. (2003). Ecology and management of wood in world rivers. In *International Conference of Wood in World Rivers (2000: Corvallis, Or.)*. American Fisheries Society.

Grissino-Mayer, H. D., & Fritts, H. C. (1997). The International Tree-Ring Data Bank: an enhanced global database serving the global scientific community. *The Holocene*, *7*(2), 235–238.

Häggblom, A. (1982). Driftwood in Svalbard as an Indicator of Sea Ice Conditions. *Geografiska Annaler. Series A, Physical Geography*, *64*(1/2), 81–94. https://doi.org/10.2307/520496

Hellmann, L., Tegel, W., Eggertsson, O., Hans Schweingruber, F., Blanchette, R., Kirdyanov, A., et al. (2013). Tracing the origin of Arctic driftwood. *Journal of Geophysical Research. Biogeosciences*, *118*(1), 68–76. Retrieved from http://cat.inist.fr/?aModele=afficheN&cpsidt=27674360

Hellmann, L., Agafonov, L., Ljungqvist, F. C., Churakova, O., Düthorn, E., Esper, J., et al. (2016). Diverse growth trends and climate responses across Eurasia's boreal forest. *Environmental Research Letters*, *11*(7), 74021.

Hellmann, L., Tegel, W., Geyer, J., Kirdyanov, A. V., Nikolaev, A. N., Eggertsson, Ó., et al. (2017). Dendro-provenancing of Arctic driftwood. *Quaternary Science Reviews*, *162*, 1–11. https://doi.org/10.1016/j.quascirev.2017.02.025

Hole, G. M., & Macias-Fauria, M. (2017). Out of the woods: Driftwood insights into Holocene pan-

Arctic sea ice dynamics. *Journal of Geophysical Research: Oceans*, *122*(9), 7612–7629. https://doi.org/10.1002/2017JC013126

Holmes, R. L. (1983). Computer-assisted quality control in tree-ring dating and measurement.

Hopkins, D. M., Smith, P. A., & Matthews, J. V. (1981). Dated wood from Alaska and the Yukon: Implications for forest refugia in Beringia. *Quaternary Research*, *15*(3), 217–249. https://doi.org/http://dx.doi.org/10.1016/0033-5894(81)90028-4

Hughes, M. K., Milsom, S. J., & Leggett, P. A. (1981). Sapwood estimates in the interpretation of tree-ring dates. *Journal of Archaeological Science*, *8*(4), 381–390.

Ingólfsson, Ó., & Landvik, J. Y. (2013). The Svalbard–Barents Sea ice-sheet – Historical, current and future perspectives. *Quaternary Science Reviews*, *64*, 33–60. https://doi.org/https://doi.org/10.1016/j.quascirev.2012.11.034

Jernas, P., Klitgaard Kristensen, D., Husum, K., Wilson, L., & Koç, N. (2013). Palaeoenvironmental changes of the last two millennia on the western and northern S valbard shelf. *Boreas*, *42*(1), 236–255.

Jones, P. D., & Mann, M. E. (2004). Climate over past millennia. *Reviews of Geophysics*, *42*(2), n/a-n/a. https://doi.org/10.1029/2003RG000143

Kinnard, C., Zdanowicz, C. M., Koerner, R. M., & Fisher, D. A. (2008). A changing Arctic seasonal ice zone: Observations from 1870–2003 and possible oceanographic consequences. *Geophysical Research Letters*, *35*(2).

Kinnard, C., Zdanowicz, C. M., Fisher, D. a., Isaksson, E., de Vernal, A., & Thompson, L. G. (2011). Reconstructed changes in Arctic sea ice over the past 1,450 years. *Nature*, *479*(7374), 509–512. https://doi.org/10.1038/nature10581

Koch, J. (2009). Improving age estimates for late Holocene glacial landforms using dendrochronology–Some examples from Garibaldi Provincial Park, British Columbia. *Quaternary Geochronology*, *4*(2), 130–139.

Kramer, N., & Wohl, E. (2017). Rules of the road: A qualitative and quantitative synthesis of large wood transport through drainage networks. *Geomorphology*, *279*, 74–97.

Kwok, R., Spreen, G., & Pang, S. (2013). Arctic sea ice circulation and drift speed: Decadal trends and ocean currents. *Journal of Geophysical Research: Oceans*, *118*(5), 2408–2425. https://doi.org/10.1002/jgrc.20191

Lehner, F., Born, A., Raible, C. C., & Stocker, T. F. (2013). Amplified Inception of European Little Ice Age by Sea Ice–Ocean–Atmosphere Feedbacks. *Journal of Climate*, *26*(19), 7586–7602. https://doi.org/10.1175/JCLI-D-12-00690.1

Linderholm, H. W., Gunnarson, B. E., Fuentes, M., Büntgen, U., & Hormes, A. (2021). The origin of driftwood on eastern and south-western Svalbard. *Polar Science*, 100658. https://doi.org/https://doi.org/10.1016/j.polar.2021.100658

MacDonald, G. M., Velichko, A. A., Kremenetski, C. V., Borisova, O. K., Goleva, A. A., Andreev, A. A., et al. (2000). Holocene treeline history and climate change across northern Eurasia. *Quaternary Research*, *53*(3), 302–311. https://doi.org/https://doi.org/10.1006/qres.1999.2123

MacDonald, G. M., Kremenetski, K. V, & Beilman, D. W. (2008). Climate change and the northern Russian treeline zone. *Philosophical Transactions of the Royal Society of London. Series B, Biological Sciences*, *363*(1501), 2285–99. https://doi.org/10.1098/rstb.2007.2200

Macias-Fauria, M., & Post, E. (2018). Effects of sea ice on Arctic biota: An emerging crisis discipline. *Biology Letters*, *14*(3), 20170702.

Macias-Fauria, M., Grinsted, A., Helama, S., Moore, J., Timonen, M., Martma, T., et al. (2010). Unprecedented low twentieth century winter sea ice extent in the Western Nordic Seas since A.D. 1200. *Climate Dynamics*, *34*(6), 781–795. https://doi.org/10.1007/s00382-009-0610-z

Maslowski, W., Clement Kinney, J., Higgins, M., & Roberts, A. (2012). The Future of Arctic Sea Ice. *Annual Review of Earth and Planetary Sciences*, *40*(1), 625–654. https://doi.org/10.1146/annurev-earth-042711-105345

McLaren, A. S. (1989). The under-ice thickness distribution of the Arctic Basin as recorded in 1958 and 1970. *Journal of Geophysical Research: Oceans (1978–2012)*, *94*(C4), 4971–4983. https://doi.org/10.1029/JC094iC04p04971

Müller, J., Werner, K., Stein, R., Fahl, K., Moros, M., & Jansen, E. (2012). Holocene cooling culminates in sea ice oscillations in Fram Strait. *Quaternary Science Reviews*, *47*, 1–14. https://doi.org/10.1016/j.quascirev.2012.04.024

Nixon, F. C., England, J. H., Lajeunesse, P., & Hanson, M. A. (2016). An 11 000-year record of driftwood delivery to the western Queen Elizabeth Islands, Arctic Canada. *Boreas*, *45*(3), 494–507. https://doi.org/10.1111/bor.12165

Norwegian Polar Institute (2014). Kartdata Svalbard 1:100 000 (S100 Kartdata) / Map Data [Data set]. Norwegian Polar Institute. https://doi.org/10.21334/npolar.2014.645336c7

Ogilvie, A. E. J., & Jónsdóttir, I. (2000). Sea ice, climate, and Icelandic fisheries in the eighteenth and nineteenth centuries. *Arctic*, *53*(4), 383–394.

Overland, J. E., & Wang, M. (2010). Large-scale atmospheric circulation changes are associated with the recent loss of Arctic sea ice. *Tellus, Series A: Dynamic Meteorology and Oceanography*, *62*(1), 1–9. https://doi.org/10.1111/j.1600-0870.2009.00421.x

Overland, J. E., Dethloff, K., Francis, J. A., Hall, R. J., Hanna, E., Kim, S.-J., et al. (2016). Nonlinear response of mid-latitude weather to the changing Arctic. *Nature Clim. Change*, *6*(11), 992–999. Retrieved from http://dx.doi.org/10.1038/nclimate3121

Owczarek, P. (2010). Dendrochronological dating of geomorphic processes in the High Arctic. *Landform Analysis*, *14*, 45–56.

Park, H., Watanabe, E., Kim, Y., Polyakov, I., Oshima, K., Zhang, X., et al. (2020). Increasing riverine heat influx triggers Arctic sea ice decline and oceanic and atmospheric warming. *Science Advances*, *6*(45), eabc4699. https://doi.org/10.1126/sciadv.abc4699

Pawłowska, J., Łącka, M., Kucharska, M., Pawlowski, J., & Zajączkowski, M. (2020). Multiproxy evidence of the Neoglacial expansion of Atlantic Water to eastern Svalbard. *Climate of the Past*, *16*(2).

Polyak, L., Alley, R. B., Andrews, J. T., Brigham-Grette, J., Cronin, T. M., Darby, D. A., et al. (2010). History of sea ice in the Arctic. *Quaternary Science Reviews*, *29*(15–16), 1757–1778. https://doi.org/10.1016/j.quascirev.2010.02.010

Post, E., & Høye, T. T. (2013). Advancing the long view of ecological change in tundra systems. *Philosophical Transactions of the Royal Society of London B: Biological Sciences*, *368*(1624). Retrieved from http://rstb.royalsocietypublishing.org/content/368/1624/20120477.abstract

Rasmussen, T. L., & Thomsen, E. (2014). Brine formation in relation to climate changes and ice retreat during the last 15,000 years in Storfjorden, Svalbard, 76–78 N. *Paleoceanography*, *29*(10), 911–929.

Rigor, I. G., Wallace, J. M., & Colony, R. L. (2002). Response of sea ice to the Arctic oscillation. *Journal of Climate*, *15*(18), 2648–2663. https://doi.org/10.1175/1520-0442(2002)015<2648:ROSITT>2.0.CO;2

Rinn, F. (2003). TSAP-Win. Time series analysis and presentation for dendrochronology and 409 related applications. *User Reference*.

Rothrock, D. A., Percival, D. B., & Wensnahan, M. (2008). The decline in arctic sea-ice thickness: Separating the spatial, annual, and interannual variability in a quarter century of submarine data. *Journal of Geophysical Research: Oceans*, *113*(5), 1–9. https://doi.org/10.1029/2007JC004252

Sander, L., Kirdyanov, A., Crivellaro, A., & Büntgen, U. (2021). Short communication: Driftwood provides reliable chronological markers in Arctic coastal deposits. *Geochronology*, *3*(1), 171–180. https://doi.org/10.5194/gchron-3-171-2021

Sarnthein, M., Van Kreveld, S., Erlenkeuser, H., Grootes, P. M., Kucera, M., Pflaumann, U., & Schulz, M. (2003). Centennial-to-millennial-scale periodicities of Holocene climate and sediment injections off the western Barents shelf, 75 N. *Boreas*, *32*(3), 447–461.

Schomacker, A., Farnsworth, W. R., Ingólfsson, Ó., Allaart, L., Håkansson, L., Retelle, M., et al. (2019). Postglacial relative sea level change and glacier activity in the early and late Holocene: Wahlenbergfjorden, Nordaustlandet, Svalbard. *Scientific Reports*, *9*(1), 6799. https://doi.org/10.1038/s41598-019-43342-z

Schweingruber, F. H. (2012). *Tree rings: basics and applications of dendrochronology*. Springer Science & Business Media.

Screen, J. a, & Simmonds, I. (2010). The central role of diminishing sea ice in recent Arctic temperature amplification. *Nature*, *464*(7293), 1334–1337. https://doi.org/10.1038/nature09051

Screen, J. a, & Simmonds, I. (2014). Amplified mid-latitude planetary waves favour particular regional weather extremes. *Nature Climate Change*, *4*(August), 704–709. https://doi.org/10.1038/NCLIMATE2271

Serreze, M. C., & Francis, J. A. (2006). The Arctic Amplification Debate. *Climatic Change*, *76*(3), 241–264. https://doi.org/10.1007/s10584-005-9017-y

Serreze, M. C., Barrett, A. P., Slater, A. G., Woodgate, R. A., Aagaard, K., Lammers, R. B., et al. (2006). The large-scale freshwater cycle of the Arctic. *Journal of Geophysical Research: Oceans*, *111*(11), 1–19. https://doi.org/10.1029/2005JC003424

Shapiro, I., Colony, R., & Vinje, T. (2003). April sea ice extent in the Barents Sea , 1850 – 2001. *Polar Research*, *22*(1), 5–10. https://doi.org/10.1111/j.1751-8369.2003.tb00089.x

Sokolov, S. Y., Svyazeva, O. A., & Kubli, V. A. (1977). Arealy Derev Ev I Kustarnikov SSSR [Ranges of Trees and Shrubs of the USSR], vol. 1. Leningrad: Nauka.

Taylor, R. E., & Aitken, M. J. (1997). *Chronometric dating in archaeology* (Vol. 2). Springer Science & Business Media.

Thompson, D. W. J., & Wallace, J. M. (1998). The Arctic oscillation signature in the wintertime geopotential height and temperature fields. *Geophysical Research Letters*, *25*(9), 1297–1300. https://doi.org/10.1029/98GL00950

Tremblay, L. -B., Mysak, L. a., & Dyke, a. S. (1997). Evidence from driftwood records for century-to-millennial scale variations of the high latitude atmospheric circulation during the Holocene. *Geophysical Research Letters*, *24*(16), 2027. https://doi.org/10.1029/97GL02028

Vavrus, S. J., Wang, F., Martin, J. E., Francis, J. A., Peings, Y., & Cattiaux, J. (2017). Changes in North American Atmospheric Circulation and Extreme Weather: Influence of Arctic Amplification and Northern Hemisphere Snow Cover. *Journal of Climate*. https://doi.org/10.1175/JCLI-D-16-0762.1

de Vernal, A., Gersonde, R., Goosse, H., Seidenkrantz, M.-S. S., & Wolff, E. W. (2013). Sea ice in the paleoclimate system: The challenge of reconstructing sea ice from proxies - an introduction. *Quaternary Science Reviews*, *79*, 1–8. https://doi.org/10.1016/j.quascirev.2013.08.009

Vinje, T. (2001). Anomalies and trends of sea-ice extent and atmospheric circulation in the Nordic Seas during the period 1864-1998. *Journal of Climate*, *14*(3), 255–267. https://doi.org/10.1175/1520-0442(2001)014<0255:AATOSI>2.0.CO;2

Walsh, J. E., Fetterer, F., Scott Stewart, J., & Chapman, W. L. (2017). A database for depicting Arctic sea ice variations back to 1850. In *Geographical Review* (Vol. 107, pp. 89–107). https://doi.org/10.1111/j.1931-0846.2016.12195.x

Wohl, E., Cadol, D., Pfeiffer, A., Jackson, K., & Laurel, D. (2018). Distribution of large wood within river corridors in relation to flow regime in the semiarid western US. *Water Resources Research*, *54*(3), 1890–1904.

Wohl, E., Kramer, N., Ruiz-Villanueva, V., Scott, D. N., Comiti, F., Gurnell, A. M., et al. (2019). The Natural Wood Regime in Rivers. *BioScience*, *69*(4), 259–273. https://doi.org/10.1093/biosci/biz013

Zeeberg, J., Lubinski, D. J., & Forman, S. L. (2001). Holocene relative sea-level history of Novaya Zemlya, Russia, and implications for Late Weichselian ice-sheet loading. *Quaternary Research*, *56*(2), 218–230.

Journal of Geophysical Research: Oceans

Supporting Information for

A driftwood-based record of Arctic sea-ice during the last 500 years from northern Svalbard reveals sea ice dynamics in the Arctic Ocean and Arctic peripheral seas

Georgia M. Hole[1], Thomas Rawson[2], Wesley R. Farnsworth[3,4], Anders Schomacker[5], Ólafur Ingólfsson[4,6], Marc Macias-Fauria[1]

[1]Biogeosciences Research Group, School of Geography and the Environment, University of Oxford, Oxford, OX1 3QY, UK.

[2]Mathematical Ecology Research Group, Department of Zoology, University of Oxford, Oxford, OX1 3SZ, UK.

[3]Nordic Volcanological Center, University of Iceland, Sturlugata 7, IS-102 Reykjavík, Iceland

[4]Department of Arctic Geology, The University Centre in Svalbard (UNIS), NO-9171, Longyearbyen Norway

[5]Department of Geosciences, UiT The Arctic University of Norway, Postboks 6050 Langnes, NO-9037 Tromsø, Norway

[6]Faculty of Earth Sciences, University of Iceland, Sturlugata 7, IS-102 Reykjavík, Iceland

Corresponding author: Georgia M. Hole (georgiamhole@gmail.com)

Contents of this file

Introduction

The supplementary information includes four figures to accompany our manuscript. Figure S1 depicts the segment lengths of 59 driftwood samples from northern Svalbard that underwent annual ring width measurements to 1/1000 mm accuracy, using LINTAB tree-ring measurement table and TSAP-Win Professional version 0.89 (Rinn, 2003). Figures S1.1-S1.4 depict the plots of samples cross-dated using TSAP-Win using a variety of parameters to assess correlation between samples. Each plot shows the ascertained best matches for samples collected from the three localities sampled in northern Svalbard – Sjuøyane, Ringhorndalen, and Vassfarbukta. Each point represents a sample's best match to a chronology. The colour of each data point displays the associated drainage basin, and the size of the point represents the CDI of the match. The density plots depict the densities of the associated time and longitude axes, weighted by the CDI of the matches. Dataset S2 includes all best matches for cross-dated TRW measures of each driftwood sample used in the study, including CDI scores and Weighted Scores, with rationale behind match choices. Dataset S3 contains all match distribution plots via the crossdating and matching methodology, with CDI and Weighted Score distribution plots for all samples.

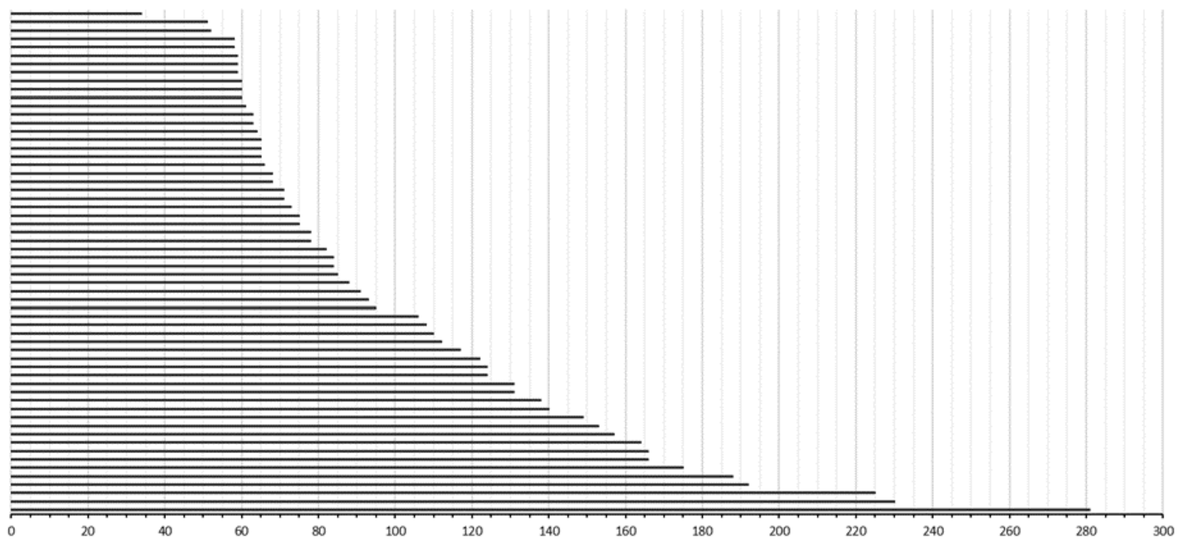

Figure S1.1. Distribution of segment lengths of measured samples, ranging from a minimum of 34 years to a maximum of 281 years.

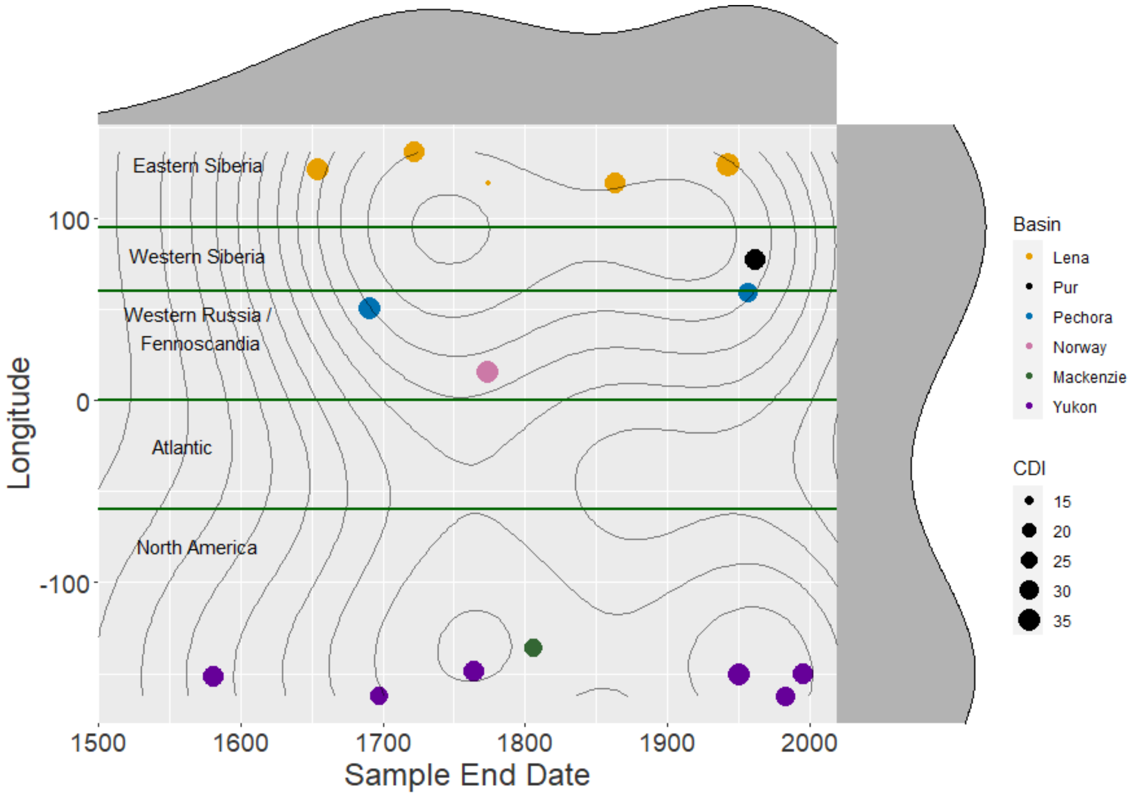

Figure S1.2. Plot of best matches for samples collected from Sjuøyane. Each point represents a sample's best match to a chronology. The colour of each data point displays the associated drainage basin, and the size of the point represents the CDI of the match. The density plots depict the densities of the associated time and longitude axes, weighted by the CDI of the matches.

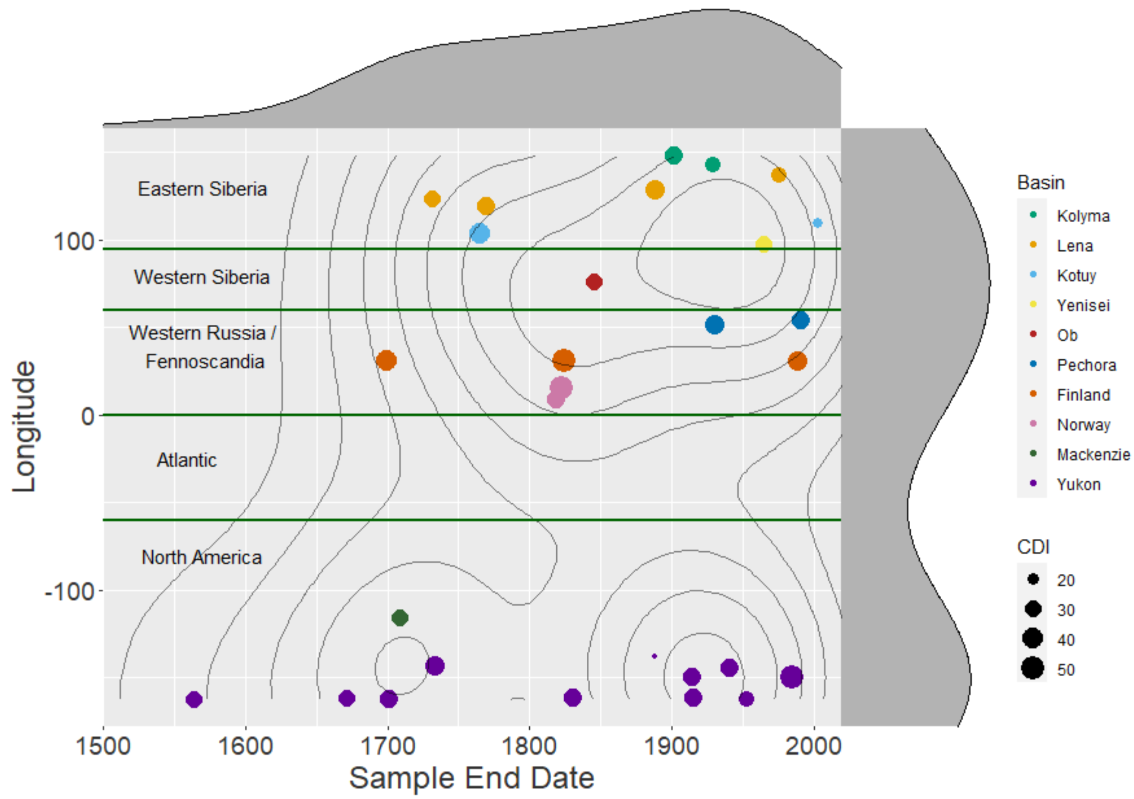

Figure S1.3. Plot of best matches for samples collected from Ringhorndalen. Each point represents a sample's best match to a chronology. The colour of each data point displays the associated drainage basin, and the size of the point represents the CDI of the match. The density plots depict the densities of the associated time and longitude axes, weighted by the CDI of the matches.

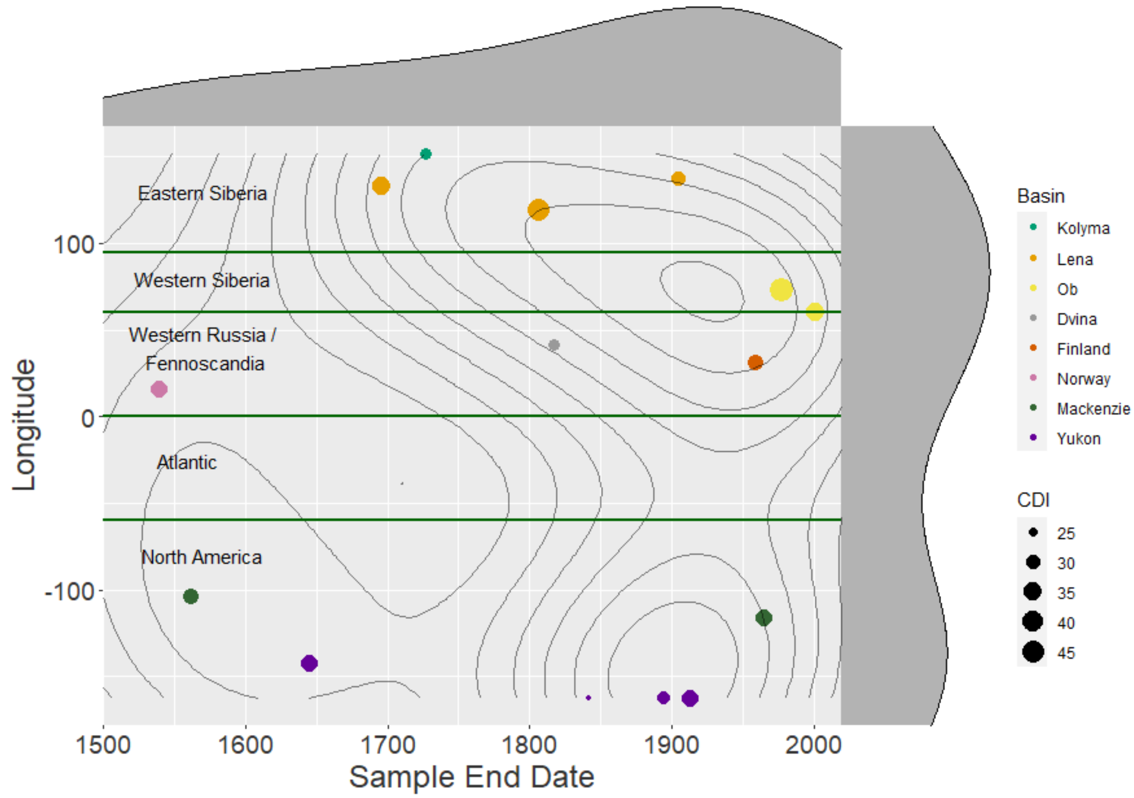

Figure S1.4. Plot of best matches for samples collected from Vassfarbukta. Each point represents a sample's best match to a chronology. The colour of each data point displays the associated drainage basin, and the size of the point represents the CDI of the match. The density plots depict the densities of the associated time and longitude axes, weighted by the CDI of the matches.

Data Set S2. All best matches including CDI scores and weighted scores, with rationale behind match choices via the study methodology, are available in dataset ds01.xlsx

Data Set S3. All match distribution plots for samples can be seen in the dataset ds02.zip. All potential matches are plotted for samples, with plots for the both the CDI scores and Weighted Score. Each point represents a match to a chronology. The colour of the point displays the associated drainage basin, and the size of the point represents either the CDI of the match, or the Weighted Score of the match, respectively. The density plots depict the densities of the associated time and longitude axes, weighted by the scores of the matches.

References

Rinn, F. (2003). TSAP-Win. Time series analysis and presentation for dendrochronology and 409 related applications. *User Reference.*